COLLEGE OF ENGINEERING

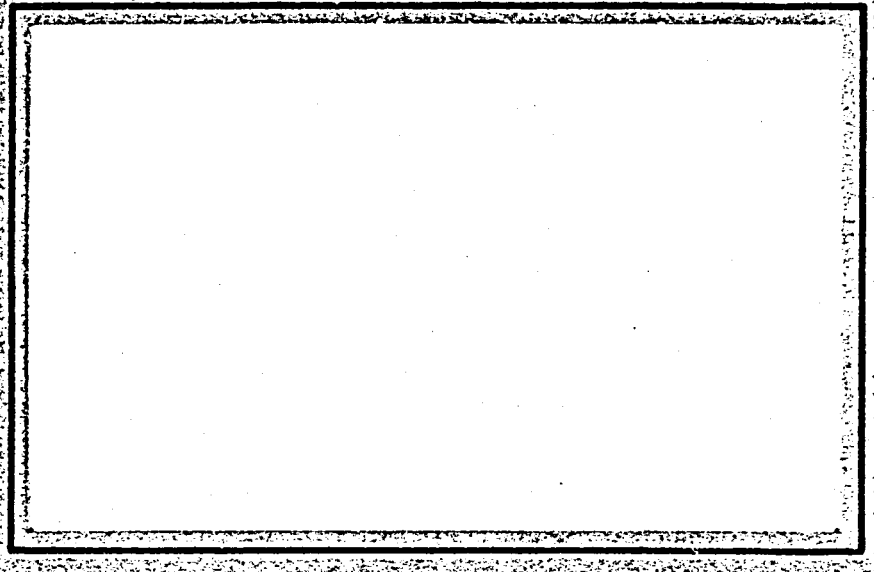

VIRGINIA POLYTECHNIC INSTITUTE AND STATE UNIVERSITY

BLACKSBURG, VIRGINIA

VPI-E-79.1

Nonparallel Stability of Two-Dimensional Nonuniformly Heated Boundary-Layers Flows

by

A. H. Nayfeh and N. M. El-Hady

Engineering Science and Mechanics Department
Virginia Polytechnic Institute and State University
Blacksburg, VA 24061

Nonparallel Stability of Two-Dimensional Nonuniformly Heated Boundary-Layer Flows

A. H. Nayfeh and N. M. El-Hady

Engineering Science and Mechanics Department,
Virginia Polytechnic Institute and State University,
Blacksburg, Virginia 24061

An analysis is presented for the linear stability of water boundary-layer flows over nonuniformly heated flat plates. Included in the analysis are disturbances due to velocity, pressure, temperature, density, and transport properties as well as variations of the liquid properties with temperature. The method of multiple scales is used to account for the nonparallelism of the mean flow. In contrast with previous analyses, the nonsimilarity of the mean flow is taken into account. No analysis agrees, even qualitatively, with the experimental data when similar profiles are used. However, both the parallel and nonparallel results qualitatively agree with the experimental results of Strazisar and Reshotko when nonsimilar profiles are used.

I. Introduction

Linke[1] was the first to investigate experimentally the effect of heat transfer on transition. He measured the drag on a vertical heated plate that is placed in a horizontal airstream. He found that heating the plate causes its drag to increase considerably. He concluded from this observation that heating the plate is destabilizing. Liepmann and Fila[2] fully confirmed the destabilizing effect of heating in air boundary layers. They performed measurements on a vertical heated plate in a horizontal airstream. They found that the critical Reynolds number decreases with wall heating. The destabilizing effect of heating in an incompressible air boundary layer is due to increasing the air viscosity next to the wall, thereby producing an inflected velocity profile. On the other hand, cooling yields a fuller velocity profile and hence a more stable flow.

Since heating decreases the viscosity of water, the above measurements and arguments suggest that heating the surface of a body in a water stream is stabilizing. This has been confirmed by the analysis of Wazzan, et al[3,4]. Their analysis is for a parallel flow and is based on the disturbance-vorticity equation only; that is, it does not include the energy equation and hence the temperature fluctuations. However, their analysis includes the effects of the mean-temperature distribution on the viscosity of the fluid. With these assumptions, Wazzan, et al[3,4] obtained a fourth-order modified Orr-Sommerfeld problem. Their results show that the critical Reynolds number increases as the wall heating increases, reaches a maximum, and then decreases. Lowell and Reshotko[5]

reformulated the parallel stability problem and included temperature as well as vorticity fluctuations. They ended up with a sixth-order rather than a fourth-order system. They found that the solutions of the fourth- and sixth-order systems are close for all wall temperature ratios over the normal liquid range of water.

The stabilizing effect of small wall-temperature ratios in water was confirmed experimentally by Strazisar, et al[6] and Parker[7]. Parker found that the transition Reynolds number for water flowing in a tube can be increased from 10×10^6 to 42×10^6 by using a 7°C wall overheat. Strazisar, et al[6] conducted an experiment for the case of uniform wall overheat. Their results show that, as the wall heating increases, the critical Reynolds number increases, the growth rates decrease, and the range of frequencies undergoing amplification decreases. All of these results qualitatively agree with the parallel stability results[3-5]. To compare quantitatively with the experimental results, El-Hady and Nayfeh[8] used the method of multiple scales to develop a nonparallel stability theory for heated water boundary layers. The nonparallel results are in good agreement with the experimental data.

Since the flow over the portion of the body upstream of the critical Reynolds number is stable, no stabilization is needed on that portion, and one would need heating only on the portions downstream of the critical Reynolds number. This suggests the use of nonuniform rather than uniform wall heating. This led Strazisar and Reshotko[9] to examine experimentally the effect of nonuniform wall heating. They conducted experiments with two types of wall heating. The first is a step change in temperatures and the second is a power-law temperature variation of

the form $T_w - T_e = Ax^n$, where T is the temperature, x is the distance in the streamwsie direction, n is a constant, and the subscripts w and e denote conditions at the wall and the edge of the boundary layer, respectively. In their power-law case, they kept $T_w(x_{ref}) - T_e$ fixed while they changed the exponent n. They made all their measurements at x_{ref}, which corresponds to a displacement-thickness Reynolds number of about 800. Their results show that decreasing n is stabilizing; that is, the case $n < 0$ results in lower growth rates than the case $n = 0$ (uniform case), which in turn results in lower growth rates than the case $n = 1$. These results could not be explained, even qualitatively, by using the parallel analyses[9,10]. This led to the speculation that an appropriate nonparallel theory may be needed to explain these results. However, applying the nonparallel theory with a similar mean flow, we were also unable to explain, even qualitatively, these results as shown in Fig. 1.

Looking closely at the aforementioned parallel and nonparallel calculations, one finds that all of them employ self-similar boundary-layer profiles. For a uniform wall temperature or for a power-law temperature distribution in a fluid having constant properties, the flow is self-similar. However, for a fluid with variable properties, the flow is not self-similar if the wall temperature is not uniform. In fact, the mean-flow measurements of Strazisar and Reshotko[9] show variations of the mean flow from the similar solution. Therefore, the purpose of the present paper is to examine the parallel and nonparallel stability of nonsimilar water boundary layers over nonuniformly heated flat plates.

II. Problem Formulation and Method of Solution

The present study is concerned with the two-dimensional, nonparallel stability of two-dimensional, viscous, heat conducting liquid boundary layers to small amplitude disturbances. The analysis takes into account variations in the fluid properties but neglects buoyancy and the dissipation energy. All fluid properties are assumed to be known functions of the temperature alone. Dimensionless quantities are introduced by using a suitable reference length L^* and the freestream values as reference quantities, where the asterisk denotes dimensional quantities.

To study the linear stability of a mean boundary-layer flow, we superpose a small time-dependent disturbance on each mean-flow, thermodynamic, and transport quantity. Thus, we let

$$\hat{q}(x,y,t) = Q_s(x,y) + q(x,y,t), \tag{1}$$

where $Q_s(x,y)$ is a mean steady quantity and $q(x,y,t)$ is an unsteady disturbance quantity. Here, q stands for the streamwise and transverse velocity components u and v, the temperature T, the pressure p, the density ρ, the specific heat c_p, the viscosity μ, and the thermal conductivity κ. Substituting Eq. (1) into the Navier-Stokes and energy equations, subtracting the mean quantities, and linearizing the resulting equations in the q's, we obtain the following disturbance equations:

$$\frac{\partial \rho}{\partial t} + \frac{\partial}{\partial x}(\rho_s u + \rho U_s) + \frac{\partial}{\partial y}(\rho_s v + \rho V_s) = 0, \tag{2}$$

$$\rho_s\left(\frac{\partial u}{\partial t} + U_s \frac{\partial u}{\partial x} + u \frac{\partial U_s}{\partial x} + V_s \frac{\partial u}{\partial y} + v \frac{\partial U_s}{\partial y}\right) + \rho\left(U_s \frac{\partial U_s}{\partial x} + V_s \frac{\partial U_s}{\partial y}\right)$$

$$= -\frac{\partial p}{\partial x} + \frac{1}{R}\left\{\frac{\partial}{\partial x}\left[\mu_s\left(r \frac{\partial u}{\partial x} + m \frac{\partial v}{\partial y}\right) + \mu\left(r \frac{\partial U_s}{\partial x} + m \frac{\partial V_s}{\partial y}\right)\right]\right.$$

$$\left. + \frac{\partial}{\partial y}\left[\mu_s\left(\frac{\partial u}{\partial y} + \frac{\partial v}{\partial x}\right) + \mu\left(\frac{\partial U_s}{\partial y} + \frac{\partial V_s}{\partial x}\right)\right]\right\}, \tag{3}$$

$$\rho_s\left(\frac{\partial v}{\partial t} + U_s \frac{\partial v}{\partial x} + u \frac{\partial V_s}{\partial x} + V_s \frac{\partial v}{\partial y} + v \frac{\partial V_s}{\partial y}\right) + \rho\left(U_s \frac{\partial V_s}{\partial x} + V_s \frac{\partial V_s}{\partial y}\right)$$

$$= -\frac{\partial p}{\partial y} + \frac{1}{R}\left\{\frac{\partial}{\partial x}\left[\mu_s\left(\frac{\partial u}{\partial y} + \frac{\partial v}{\partial x}\right) + \mu\left(\frac{\partial U_s}{\partial y} + \frac{\partial V_s}{\partial x}\right)\right]\right.$$

$$\left. + \frac{\partial}{\partial y}\left[\mu_s\left(r \frac{\partial v}{\partial y} + m \frac{\partial u}{\partial x}\right) + \mu\left(r \frac{\partial V_s}{\partial y} + m \frac{\partial U_s}{\partial x}\right)\right]\right\}, \tag{4}$$

$$\rho_s\left[\frac{\partial T}{\partial t} + u \frac{\partial T_s}{\partial x} + U_s \frac{\partial T}{\partial x} + v \frac{\partial T_s}{\partial y} + V_s \frac{\partial T}{\partial y}\right] + \left(\rho_s \frac{c_p}{c_{p_s}} + \rho\right)\left[U_s \frac{\partial T_s}{\partial x}\right.$$

$$\left. + V_s \frac{\partial T_s}{\partial y}\right] = \frac{1}{RPr_e c_{p_s}} \frac{\partial}{\partial x}\left(\kappa_s \frac{\partial T}{\partial x} + \kappa \frac{\partial T_s}{\partial x}\right] + \frac{\partial}{\partial y}\left(\kappa_s \frac{\partial T}{\partial y}\right.$$

$$\left. + \kappa \frac{\partial T_s}{\partial y}\right) \quad , \tag{5}$$

$$\rho,\ \mu,\ \kappa,\ c_p = \left[\frac{d\rho_s}{dT_s}, \frac{d\mu_s}{dT_s}, \frac{d\kappa_s}{dT_s}, \frac{dc_{p_s}}{dT_s}\right] T \quad . \tag{6}$$

Here, c_{p_s} is the liquid specific heat at constant pressure, $R = \rho_e^* U_e^* L^*/\mu_e^*$ is the Reynolds number, and $Pr_e = c_{p_e}^* \mu_e^*/\kappa_e^*$ is the freestream Prandtl number. Moreover,

$$r = \frac{2}{3}(\ell + 2),\ m = \frac{2}{3}(\ell - 1),\ f = \frac{1}{3}(1 + 2\ell),\ \lambda = \frac{2}{3}(\ell - 1), \tag{7}$$

where ℓ is the ratio of the second to the first viscosity coefficients ($\ell = 0$ is the Stokes assumption).

The problem is completed by the specification of the boundary conditions; they are

$$u = v = T = 0 \text{ at } y = 0, \tag{8}$$

$$u, v, T \to 0 \quad \text{as } y \to \infty. \tag{9}$$

We restrict our analysis to mean flows that are slightly nonparallel; that is, the transverse velocity component is small compared with respect to the streamwise velocity component. This condition demands all mean-flow variables to be weak functions of the streamwise position. These assumptions are expressed mathematically by writing the mean-flow variables in the form

$$U_s = U_s(x_1, y), \quad V_s = \varepsilon \tilde{V}_s(x_1, y), \quad P_s = P_s(x_1), \quad T_s = T_s(x_1, y), \tag{10}$$

where $x_1 = \varepsilon x$ with ε being a small dimensionless parameter characterizing the nonparallelism of the mean flow. In what follows, we drop the carrot from V_s.

To determine an approximate solution to Eqs. (2)-(10), we use the method of multiple scales[11] and seek a first-order expansion for the disturbance variables u, v, p, and T in the form of a traveling harmonic wave; that is, we expand each disturbance flow quantity in the form

$$q(x_1, y, t) = [q_0(x_1, y) + \varepsilon q_1(x_1, y) + \ldots]\exp(i\theta), \tag{11}$$

where

$$\frac{\partial \theta}{\partial x} = \alpha_0(x_1), \quad \frac{\partial \theta}{\partial t} = -\omega. \tag{12}$$

$\theta = \alpha_0 x - \omega t$

For the case of spatial stability, α_0 is the complex wavenumber for the quasi-parallel flow problem and ω is the disturbance angular frequency, which is taken to be real.

Substituting Eqs. (11) and (12) into Eqs. (2)-(10), transforming the time and spatial derivatives from t and x to θ and x_1, and equating the coefficients of ε^0 and ε on both sides, we obtain problems describing the q_0 and q_1 flow quantities. These problems are referred to as the zeroth- and first-order problems and they are solved in the next two sections.

III. The Zeroth-Order Problem

Substituting Eqs. (11) and (12) into Eqs. (2)-(10) and equating the coefficients of ε^n on both sides, we obtain the follcwing problem:

$$L_1(u_0,v_0,p_0,T_0) = i\alpha_0[\rho_s u_0 + (U_s - \frac{\omega}{\alpha_0})\rho_0] + \frac{\partial}{\partial y}(\rho_s v_0) = 0, \quad (13)$$

$$L_2(u_0,v_0,p_0,T_0) = [i\rho_s\alpha_0(U_s - \frac{\omega}{\alpha_0}) + \frac{r}{R}\mu_s\alpha_0^2]u_0 + (\rho_s \frac{\partial U_s}{\partial y} - \frac{i}{R}\frac{\partial \mu_s}{\partial y}\alpha_0)v_0 + i\alpha_0 p_0 - \frac{T_0}{R}\frac{\partial}{\partial y}(\frac{d\mu_s}{dT_s}\frac{\partial U_s}{\partial y}) - \frac{1}{R}\frac{\partial \mu_s}{\partial y}\frac{\partial u_0}{\partial y} - \frac{if}{R}\mu_s\alpha_0\frac{\partial v_0}{\partial y} - \frac{1}{R}\frac{d\mu_s}{dT_s}\frac{\partial U_s}{\partial y}\frac{\partial T_0}{\partial y} - \frac{1}{R}\mu_s\frac{\partial^2 u_0}{\partial y^2} = 0, \quad (14)$$

$$L_3(u_0,v_0,p_0,T_0) = [i\rho_s\alpha_0(U_s - \frac{\omega}{\alpha_0}) + \frac{1}{R}\mu_s\alpha_0^2]v_0 - \frac{im}{R}\alpha_0\frac{\partial \mu_s}{\partial y}u_0 - \frac{i}{R}\alpha_0\frac{d\mu_s}{dT_s}\frac{\partial U_s}{\partial y}T_0 - \frac{if}{R}\mu_s\alpha_0\frac{\partial u_0}{\partial y} - \frac{r}{R}\frac{\partial \mu_s}{\partial y}\frac{\partial v_0}{\partial y} + \frac{\partial p_0}{\partial y} - \frac{r}{R}\mu_s\frac{\partial^2 v_0}{\partial y^2} = 0, \quad (15)$$

$$L_4(u_0,v_0,p_0,T_0) = [i\rho_s\alpha_0(U_s - \frac{\omega}{\alpha_0}) + \frac{1}{RPr_e c_{p_s}}(\kappa_s\alpha_0^2 - \frac{\partial^2 \kappa_s}{\partial y^2})]T_0 + \rho_s\frac{\partial T_s}{\partial y}v_0 - \frac{2}{RPr_e c_{p_s}}\frac{\partial \kappa_s}{\partial y}\frac{\partial T_0}{\partial y} - \frac{1}{RPr_e c_{p_s}}\kappa_0\frac{\partial^2 T_0}{\partial y^2} = 0. \quad (16)$$

The boundary conditions are:

$$u_0 = v_0 = T_0 = 0 \qquad \text{at } y = 0, \quad (17)$$

$$u_0,\ v_0,\ T_0 \to 0 \qquad \text{as } y \to \infty. \quad (18)$$

Equations (13)-(18) constitute an eigenvalue problem, which is solved numerically. It is convenient to express it as a set of six first-order equations by introducing the new variables z_{0n} defined by

$$z_{01} = u_0, \qquad z_{02} = \frac{\partial u_0}{\partial y}, \qquad z_{03} = v_0,$$

$$z_{04} = p_0, \qquad z_{05} = T_0, \qquad z_{06} = \frac{\partial T_0}{\partial y}. \tag{19}$$

Then, Eqs. (13)-(18) can be rewritten in the compact form

$$\frac{\partial z_{0i}}{\partial y} - \sum_{j=1}^{6} a_{ij} z_{0j} = 0 \quad \text{for } i = 1,2..,6, \tag{20}$$

$$z_{01} = z_{03} = z_{05} = 0 \qquad \text{at } y = 0, \tag{21}$$

$$z_{01},\ z_{03},\ z_{05} \to 0 \qquad \text{as } y \to \infty, \tag{22}$$

where the a_{ij} are the elements of a 6 x 6 variable-coefficient matrix. The nineteen nonzero elements of this matrix are listed in Appendix I.

To set up the numerical solution, we first replace the boundary conditions (22) by a new set at $y = y_e$ where y_e is a convenient location outside the boundary layer. Outside the boundary layer, the mean flow is independent of y and the coefficients a_{ij} are constants. Hence, the general solution of Eqs. (20) can be expressed in the form

$$z_{0i} = \sum_{j=1}^{6} \Lambda_{ij} c_j \exp(\lambda_j y) \quad \text{for } i = 1,2,\ldots,6,\ y = y_e \tag{23}$$

where the λ_j are the eigenvalues of the matrix $[a_{ij}]$, the Λ_{ij} are the elements of the corresponding eigenvector matrix, and the c_j are arbitrary constants. The real parts of three of the λ_j are negative, while the real parts of the remaining λ_j are positive. Let us order these eigenvalues so that the real parts of λ_1, λ_2, and λ_3 are negative. Then, the boundary condition (22) demands that c_4, c_5, and c_6 are zero. To set up this condition for the numerical procedure, we first solve Eqs. (23) for the $c_j \exp(\lambda_j y)$ and obtain

$$c_j \exp(\lambda_j y) = \sum_{i=1}^{6} b_{ij} z_{0i} \quad \text{for } j = 1,2,\ldots,6, \tag{24}$$

where the matrix $[b_{ij}]$ is the inverse of $[\Lambda_{ij}]$. Setting $c_4=c_5=c_6 = 0$ in Eq. (24) leads to

$$\sum_{i=1}^{6} b_{ij} z_{0i} = 0 \quad \text{for } j = 4,5, \text{ and } 6 \quad \text{at } y = y_e. \tag{25}$$

Using Eqs. (25) as the boundary condition at $y = y_e$ and guessing a value for α_0, we integrate Eqs. (20) from $y = y_e$ to $y = 0$ by using the computer program developed by Scott and Watts[12] that employs a Gram-Schmidt orthonormalization procedure, and then we attempt to satisfy the boundary conditions (21). If the guessed value for α_0 is the correct eigenvalue, the three boundary conditions will be satisfied. In general, the guessed value is not the correct value and the boundary conditions at the wall are not satisfied. A Newton-Raphson procedure is used to update the value of α_0 and the integration is repeated until the wall-boundary conditions are satisfied to within a prescribed accuracy. This leads to a value for α_0 and the eigenfunctions are recovered using the stored solution vectors. They can be expressed in the form

$$z_{0i} = A(x_1)\zeta_i(x_1,y) \quad \text{for } i = 1,2,\ldots,6, \tag{26}$$

where A is still an undetermined function at this level of approximation. It is determined by imposing the solvability condition at the next level of approximation.

IV. The First-Order Problem

With the solution of the zeroth-order problem given by Eq. (26), the first-order problem becomes

$$\frac{\partial z_{1i}}{\partial y} - \sum_{j=1}^{6} a_{ij} z_{1j} = G_i \frac{dA}{dx_1} + D_i A \quad \text{for } i = 1,2,\ldots,6, \tag{27}$$

$$z_{11} = z_{13} = z_{15} = 0 \qquad \text{at } y = 0\ , \tag{28}$$

$$z_{11},\ z_{13},\ z_{15} \to 0 \qquad \text{as } y \to \infty\ , \tag{29}$$

where the G_i and D_i are known functions of the ζ_i, α_0, and the mean-flow quantities. They are defined in Appendix II.

Since the homogeneous parts of Eqs. (27)-(29) are the same as Eqs. (20)-(22) and since the latter have a nontrivial solution, the inhomogeneous Eqs. (27)-(29) have a solution if, and only if, a solvability condition is satisfied. In this case, the solvability condition demands the inhomogeneities to be orthogonal to every solution of the adjoint homogeneous problem; that is,

$$\int_0^\infty \sum_{i=1}^{6} \left[G_i \frac{dA}{dx_1} + D_i A\right] W_i\, dy = 0, \tag{30}$$

where the $W_i(x_1,y)$ are the solutions of the adjoint homogeneous problem corresponding to the eigenvalue α_0. Thus, they are the solutions of

$$\frac{\partial W_i}{\partial y} + \sum_{j=1}^{6} a_{ji} W_j = 0 \text{ for } i = 1,2,\ldots,6, \tag{31}$$

$$W_2 = W_4 = W_6 = 0 \qquad \text{at } y = 0, \tag{32}$$

$$W_2,\ W_4,\ W_6 \to 0 \qquad \text{as } y \to \infty, \tag{33}$$

Substituting for the G_i and D_i from Appendix II into Eq. (30), we obtain the following equation for the evolution of the amplitude A:

$$\frac{1}{A}\frac{dA}{dx_1} = i\alpha_1(x_1), \tag{34}$$

where

$$i\alpha_1 = -\left[\int_0^\infty \sum_{j=1}^{6} D_j W_j dy\right] / \left[\int_0^\infty \sum_{j=1}^{6} G_j W_j dy\right]. \tag{35}$$

The solution of Eq. (34) can be written as

$$A = A_0 \exp\left[i\epsilon \int \alpha_1(x_1) dx\right], \tag{36}$$

where A_0 is a constant of integration.

To determine $\alpha_1(x_1)$, we need to evaluate $d\alpha_0/dx_1$ and the $\partial\zeta_i/\partial x_1$. To accomplish this, we differentiate Eqs. (20)-(22) with respect to x_1 and obtain

$$\frac{\partial}{\partial y}\left(\frac{\partial \zeta_i}{\partial x_1}\right) - \sum_{j=1}^{6} a_{ij}\left(\frac{\partial \zeta_j}{\partial x_1}\right) = G_i \frac{d\alpha_0}{dx_1} + S_i \text{ for } i = 1,2,\ldots,6, \tag{37}$$

$$\frac{\partial \zeta_1}{\partial x_1} = \frac{\partial \zeta_3}{\partial x_1} = \frac{\partial \zeta_5}{\partial x_1} = 0 \text{ at } y = 0, \tag{38}$$

$$\frac{\partial \zeta_1}{\partial x_1}, \frac{\partial \zeta_3}{\partial x_1}, \frac{\partial \zeta_5}{\partial x_1} \to 0 \text{ as } y \to \infty. \tag{39}$$

The initial conditions for the computational procedures are chosen to exclude any multiple of the homogeneous solutions. The S_i and G_i are known functions of ζ_i, α_0, and the mean-flow quantities and their derivatives; they are given by

$$S_i = \sum_{j=1}^{6} \zeta_j \left.\frac{\partial a_{ij}}{\partial x_1}\right|_{\alpha_0} \text{ and } G_i = \sum_{j=1}^{6} \zeta_j \frac{\partial a_{ij}}{\partial \alpha_0} \text{ for } i = 1,2,\ldots,6 \tag{40}$$

Using the solvability condition of Eqs. (37)-(39), we find that

$$\frac{d\alpha_0}{dx_1} = -\left[\int_0^\infty \sum_{i=1}^{6} S_i W_i dy\right] / \left[\int_0^\infty \sum_{i=1}^{6} G_i W_i dy\right]. \tag{41}$$

Therefore, to the first approximation

$$z_{01} = A_0\zeta_1(x_1,y)\exp[i\int(\alpha_0 + \varepsilon\alpha_1)dx - i\omega t] + O(\varepsilon), \qquad (42)$$

where the z_{0i} are related to the disturbance variables by Eq. (19) and the constant A_0 is determined from the initial conditions. It is clear from Eq. (42) that, in addition to the dependence of the eigensolutions on x_1, the eigenvalue α_0 is modified by $\varepsilon\alpha_1$. The present solution reduces to those obtained by Nayfeh, et al[13] and Saric and Nayfeh[14] for the case of nonheat conducting flows.

V. The Mean Flow

For flows whose thermodynamic and transport properties are functions of temperature, the two-dimensional boundary-layer equations for a zero-pressure gradient and in boundary-layer coordinates are

$$\frac{\partial}{\partial x}(\rho u) + \frac{\partial}{\partial \bar{y}}(\rho \bar{v}) = 0 \quad , \tag{43}$$

$$\rho u \frac{\partial u}{\partial x} + \rho \bar{v} \frac{\partial u}{\partial \bar{y}} = \frac{\partial}{\partial \bar{y}}\left(\mu \frac{\partial u}{\partial y}\right), \tag{44}$$

$$\rho u c_p \frac{\partial T}{\partial x} + \rho \bar{v} c_p \frac{\partial T}{\partial \bar{y}} = \frac{\partial}{\partial \bar{y}}\left(\kappa \frac{\partial T}{\partial \bar{y}}\right) \quad , \tag{45}$$

The temperature dependence of ρ and μ couples the momentum and energy equations. Note that buoyancy and viscous dissipation effects are neglected.

We introduce the Levy-Lees transformation[15]

$$d\xi = \rho_e U_e \mu_e dx \quad , \tag{46}$$

$$d\eta = \rho U_e (2\xi)^{-1/2} d\bar{y} \quad . \tag{47}$$

Then, the derivatives with respect to x and $\bar{y}$ are transformed according to

$$\frac{\partial}{\partial x} = \rho_e U_e \mu_e \frac{\partial}{\partial \xi} + \frac{\partial \eta}{\partial x}\frac{\partial}{\partial \eta} \quad , \tag{48}$$

$$\frac{\partial}{\partial \bar{y}} = \frac{\rho U_e}{(2\xi)^{1/2}}\frac{\partial}{\partial \eta} \quad . \tag{49}$$

Substituting Eqs. (48) and (49) into Eqs. (43)-(45) yields

$$2\xi \frac{\partial U}{\partial \xi} + \frac{\partial V}{\partial \eta} + U = 0, \tag{50}$$

$$2\xi U \frac{\partial U}{\partial \xi} + V \frac{\partial U}{\partial \eta} - \frac{\partial}{\partial \eta}\left(C \frac{\partial U}{\partial \eta}\right) = 0, \tag{51}$$

$$2\xi U \frac{\partial H}{\partial \xi} + V \frac{\partial H}{\partial \eta} - \frac{\partial}{\partial \eta}\left(\frac{C}{Pr} \frac{\partial H}{\partial \eta}\right) = 0, \tag{52}$$

where

$$U = u/U_e, \; H = T/T_e \; , \tag{53}$$

$$V = \frac{2\xi}{\rho_e U_e \mu_e}\left[U \frac{\partial \eta}{\partial x} + \frac{\rho \bar{v}}{2(\xi)^{1/2}}\right], \tag{54}$$

$$C = \rho\mu/\rho_e\mu_e, \; Pr = c_p\mu/\kappa \; . \tag{55}$$

The boundary conditions are

$$U(\xi,0) = 0, \quad V(\xi,0) = 0, \; H(\xi,0) = H_w(\xi), \tag{56}$$

$$U(\xi,\eta) \to 1 \text{ and } H(\xi,\eta) \to 1 \text{ as } \eta \to \eta_e. \tag{57}$$

Equations (50)-(52), (56), and (57) are numerically integrated using a step by step procedure in the streamwise direciton. A three-point implicit finite-difference technique is used to reduce the energy and momentum equations and the boundary conditions to a set of simultaneous tridiagonal equations. These equations are linearized and then solved by using the algorithm of Thomas. Then, the continuity equation is numerically integrated by using the trapezoidal rule. The method of solution closely parallels those of Flügge-Lotz and Blottner[16], Davis and Flügge-Lotz[17], and Harris[18].

VI. Analytical Results and Comparison with Experiments

Strazisar and Reshotko[9] performed their experiments in a water tunnel whose test section was 394 mm long, 229 mm wide, and 152 mm high. The freestream turbulence was 0.1 - 0.2% for $U_e^* < 3.4$ m/s. They measured the boundary-layer characteristics on a flat plate that was 348 mm long and 16 mm thick and spanned the test section. The plate was fitted with a rounded leading edge (0.79 mm radius) located 10.8 mm below the top of the test section.

Disturbances were artificially introduced in the boundary layer by using a vibrating ribbon that is stretched across the plate surface 95.3 mm behind the leading edge. The amplitudes of the generated disturbances were measured at five stations spaced 6.4 mm apart between x = 127 mm and x = 152.4 mm. They traversed the boundary layer in the normal direction and recorded the peak amplitude. Then, they determined the growth rates at x = 139.7 mm by using a polynomial curve fit of the peak amplitude data.

The plate heating was provided by 11 electric heaters distributed along the plate. The wall temperature was monitored by using 11 thermistors imbedded in the surface of the plate at its centerline. However, because of the large temperature gradients involved, the thermistors did not accurately yield the plate temperature. Consequently, they had to determine the wall temperature from boundary-layer profiles measured with a hot-film anemometer operating as a resistance thermometer. Due to equipment limitations, the wall temperature could not be monitored or maintained near the leading edge. Since the thermal boundary is very thin near the leading edge, measurement of temperature

profiles using the hot-film anemometer were impractical in that region and the first measurement of the wall temperature was provided by a thermistor imbedded 30.5 mm from the leading edge.

In the case of the power-law distribution $T_w - T_e = Ax^n$, Strazisar and Reshotko held the temperature difference fixed at $x_{ref.}$, while they varied n and x as shown in Fig. 2. They presented growth data at $x_{ref.}$ = 139.7 mm only (corresponding to R = 475). Their results show that decreasing n is stabilizing. However, Fig. 1 shows that decreasing n is destabilizing in both the parallel and nonparallel calculations when a similar mean flow is used. Hence, using self-similar mean profiles cannot predict the experimental data.

Since the upstream wall temperature distribuiton is essential for calculating nonsimilar boundary layers we are unable to compare quantitatively the analytical results with the data of Strazisar and Roshotko for the case of power-law distributions. Figures 3-5 show the variation of the parallel and nonparallel growth rates with frequency (defined as $F = \omega^* \nu_e^* / U_e^{*2}$) calculated for the power-law distributions shown in Fig. 2 for ΔT = 1.67°, 2.78°, and 4.44°C at $x_{ref.}$ = 139.7 mm. In each figure, we show the results for n = -0.5, 0, and 1 as well as the results for the unheated case. The nonparallel growth rates do not include the distortion effect of the mode shape. Including this distortion modifies quantitatively but not qualitatively the results. Both parallel and nonparallel theories predict that decreasing the exponent n results in a stabilizing effect at $x_{ref.}$, in qualitative agreement with the experimental results[9].

The stabilizing effect produced by decreasing the exponent n can be explained as follows. As n decreases, Fig. 2 shows that ΔT increases

at all locations upstream of $x_{ref.}$. But increasing ΔT results in a fuller velocity profile and hence a more stable flow. Therefore, the stabilizing effect produced at $x_{ref.}$ is a cumulative of all upstream stabilizing effects. However, as n decreases, ΔT decreases downstream of $x_{ref.}$, resulting in less fuller velocity profiles. Therefore, at some location downstream of $x_{ref.}$, a distribution with a larger exponent will be more stabilizing as shown in Fig. 6. Thus the neutral stability curves are not nested and conclusions regarding stabilizing and destabilizing effects away from $x_{ref.}$ depend on the Reynolds number. The integration of the growth rates yields the amplification factor, which seems to be the best indicator of stability. Figure 7 shows the variation of the integrated growth rates of Fig. 6 with Reynolds number. Also shown is the variation of the maximum amplification factor with the exponent n. It appears that the maximum amplification factor for n = - 0.5 and n=0 are nearly the same, while it is higher for n = 1. This result holds for other frequencies as indicated by the nesting of the growth-rate curves (Fig. 4) as functions of frequency.

VII. Conclusion

We analyze the linear nonparallel stability of two-dimensional liquid boundary layers on a flat plate for the case of nonuniform wall heating. Stability calculations using a self-similar mean flow cannot predict, even qualitatively, the experimental results of Strazisar and Reshotko for power-law temperature distributions. However, by using nonsimilar mean flows, both parallel and nonparallel results are in qualitative agreement with the experiments. The stabilizing and destabilizing effects at $x_{ref.}$ depend on the temperature distribution.

Acknowledgments

The comments and suggestions of Dr. W. S. Saric are greatly appreciated. This work is supported by the United States National Aeronautics and Space Administration, Langley Research Center Grant No. NSG-1255.

References

1. W. Linke, Luftfahrtforschung 19, 157 (1942).
2. H. W. Liepmann and G. H. Fila, NACA TN 890 (1947).
3. A. R. Wazzan, T. T. Okamura, and A. M. O. Smith, Trans. ASME C 90, 109 (1968).
4. A. R. Wazzan, T. T. Okamura, and A. M. O. Smith, in Proc. 4th Int. Heat Transfer Conf. (Elsevier, Paris, 1970), U. Grigull and E. Hahne, Eds., 2, FC 1.4.
5. R. L. Lowell and E. Reshotko, Case Western Reserve Univ. Report FTAS/TR-73-95, 1974.
6. A. J. Strazisar, E. Reshotko, and J. M. Prahl, J. Fluid Mech. 83, 225 (1977).
7. S. J. Parker, in Proc. Twelfth Symposium on Naval Hydrodynamics (National Academy of Sciences, Washington, D. C., 1978), to be published.
8. N. M. El-Hady and A. H. Nayfeh, in Proc. Twelfth Symposium on Naval Hydrodynamics (National Academy of Sciences, Washington, D.C., 1978), to be published.
9. A. J. Strazisar and E. Reshotko, Phys. Fluids 21, 727 (1978).
10. A. R. Wazzan and C. Gazley, in Proc. 2nd Int. Conf. Drag Reduction (Cambridge, 1977), Paper No. E3.
11. A. H. Nayfeh, Perturbation Methods (Wiley-Interscience, New York, 1973), Chap. 6.
12. M. R. Scott and H. A. Watts, SIAM, J. Numer. Analysis 14, 40 (1977).
13. A. H. Nayfeh, W. S. Saric, and D. T. Mook, Arch. Mech. Stosow 26, 401 (1974).

14. W. S. Saric and A. H. Nayfeh, Phys. Fluids 18, 945 (1975).

15. L. Lees, Jet Propulsion 26, 259 (1956).

16. I. Flügge-Lotz and F. G. Blottner, Rep. AFOSR 2206, U. S. Air Force (1962).

17. R. T. Davis and I. Flügge-Lotz, Tech. Rep. No. 143, Div. Eng. Mech., Stanford Univ. (1963).

18. J. E. Harris, Ph.D. Thesis, Virginia Polytechnic Institute and State Universtiy (1970).

APPENDIX I

$$a_{12} = 1,$$

$$a_{21} = \frac{i\rho_s \alpha_0 R}{\mu_s}\left(U_s - \frac{\omega}{\alpha_0}\right) + \alpha_0^2,$$

$$a_{22} = -\frac{1}{\mu_s}\frac{\partial \mu_s}{\partial y},$$

$$a_{23} = \frac{\rho_s R}{\mu_s}\frac{\partial U_s}{\partial y} - i\alpha_0\left(\frac{1}{\mu_s}\frac{\partial \mu_s}{\partial y} - \frac{f}{\rho_s}\frac{\partial \rho_s}{\partial y}\right),$$

$$a_{24} = \frac{i\alpha_0 R}{\mu_s},$$

$$a_{25} = -\frac{f\alpha_0^2}{\rho_s}\frac{d\rho_s}{dT_s}\left(U_s - \frac{\omega}{\alpha_0}\right) - \frac{1}{\mu_s}\frac{\partial}{\partial y}\left(\frac{d\mu_s}{dT_s}\frac{\partial U_s}{\partial y}\right),$$

$$a_{26} = -\frac{1}{\mu_s}\frac{d\mu_s}{dT_s}\frac{\partial U_s}{\partial y},$$

$$a_{31} = -i\alpha_0,$$

$$a_{33} = -\frac{1}{\rho_s}\frac{\partial \rho_s}{\partial y},$$

$$a_{35} = -\frac{i\alpha_0}{\rho_s}\frac{d\rho_s}{dT_s}\left(U_s - \frac{\omega}{\alpha_0}\right),$$

$$a_{41} = -\frac{i\alpha_0 \mu_s}{R}\left(\frac{2}{\mu_s}\frac{\partial \mu_s}{\partial y} - \frac{r}{\rho_s}\frac{\partial \rho_s}{\partial y}\right),$$

$$a_{42} = -\frac{i\alpha_0 \mu_s}{R},$$

$$a_{43} = \frac{\alpha_0 \mu_s}{R}\left\{-\alpha_0 - \frac{r}{\alpha_0 \mu_s \rho_s}\frac{\partial \mu_s}{\partial y}\frac{\partial \rho_s}{\partial y} - \frac{r}{\alpha_0 \rho_s}\left[\frac{\partial^2 \rho_s}{\partial y^2} - \frac{2}{\rho_s}\left(\frac{\partial \rho_s}{\partial y}\right)^2\right] - \frac{i\rho_s R}{\mu_s}\left(U_s - \frac{\omega}{\alpha_0}\right)\right\},$$

$$a_{45} = \frac{i\alpha_0 \mu_s}{R}\left\{\frac{1}{\mu_s}\frac{d\mu_s}{dT_s}\frac{\partial U_s}{\partial y} - \frac{r}{\mu_s \rho_s}\frac{d\rho_s}{dT_s}\frac{\partial \mu_s}{\partial y}\left(U_s - \frac{\omega}{\alpha_0}\right) - \frac{r}{\rho_s}\left[\frac{d\rho_s}{dT_s}\frac{\partial U_s}{\partial y} + \left(U_s - \frac{\omega}{\alpha_0}\right)\left(\frac{\partial}{\partial y}\frac{d\rho_s}{dT_s} - \frac{2}{\rho_s}\frac{d\rho_s}{dT_s}\frac{\partial \rho_s}{\partial y}\right)\right]\right\},$$

$$a_{46} = -\frac{i\alpha_0 \mu_s r}{R\rho_s} \frac{d}{dT_s}\left(U_s - \frac{\omega}{\alpha_0}\right),$$

$$a_{56} = 1,$$

$$a_{63} = \frac{RPr_e c_{p_s} \rho_s}{\kappa_s} \frac{\partial T_s}{\partial y},$$

$$a_{65} = \frac{iRPr_e c_{p_s} \alpha_0 \rho_s}{\kappa_s}\left(U_s - \frac{\omega}{\alpha_0}\right) + \alpha_0^2 - \frac{1}{\kappa_s}\frac{\partial^2 \kappa_s}{\partial y^2},$$

$$a_{66} = -\frac{2}{\kappa_s}\frac{\partial \kappa_s}{\partial y}.$$

APPENDIX II

$$G_1 \frac{dA}{dx_1} + D_1 A = 0,$$

$$G_2 \frac{dA}{dx_1} + D_2 A = - \frac{if\alpha_0}{\rho_s} I_m - \frac{R}{\mu_0} I_x,$$

$$G_3 \frac{dA}{dx_1} + D_3 A = \frac{1}{\rho_s} I_m,$$

$$G_4 \frac{dA}{dx_1} + D_4 A = \frac{r}{R} \frac{\mu_s}{\rho_s} \left(\frac{1}{\mu_s} \frac{\partial \mu_s}{\partial y} - \frac{2}{\rho_s} \frac{\partial \rho_s}{\partial y}\right) I_m + \frac{r}{R} \frac{\mu_s}{\rho_s} \frac{\partial}{\partial y} I_m + I_y,$$

$$G_5 \frac{dA}{dx_1} + D_5 A = 0,$$

$$G_6 \frac{dA}{dx_1} + D_6 A = - \frac{RPr_e c_{p_s}}{\kappa_s} I_e,$$

where

$$I_m = - \left[\rho_s \zeta_1 + U_s \frac{d\rho_s}{dT_s} \zeta_5\right] \frac{dA}{dx_1} - \left\{\frac{\partial \rho_s}{\partial x_1} \zeta_1 + \rho_s \frac{\partial \zeta_1}{\partial x_1} + \left[\frac{d\rho_s}{dT_s} \left(\frac{\partial U_s}{\partial x_1} + \frac{\partial V_s}{\partial y}\right) + U_s \frac{\partial}{\partial x_1} \left(\frac{d\rho_s}{dT_s}\right) + V_s \frac{\partial}{\partial y} \left(\frac{d\rho_s}{dT_s}\right)\right] \zeta_5 + U_s \frac{d\rho_s}{dT_s} \frac{\partial \zeta_5}{\partial x_1} + V_s \frac{d\rho_s}{dT_s} \frac{\partial \zeta_5}{\partial y}\right\} A,$$

$$I_x = \left[\left(\frac{2ir}{R} \mu_s \alpha_0 - \rho_s U_s\right) \zeta_1 + \frac{1}{R} \frac{\partial \mu_s}{\partial y} \zeta_3 + \frac{f}{R} \mu_s \frac{\partial \zeta_3}{\partial y} - \zeta_4\right] \frac{dA}{dx_1}$$

$$+ \left\{\left[\frac{ir}{R} \left(\mu_s \frac{d\alpha_0}{dx_1} + \alpha_0 \frac{\partial \mu_s}{\partial x_1}\right) - \rho_s \frac{\partial U_s}{\partial x_1}\right] \zeta_1 + \left(\frac{2ir}{R} \mu_s \alpha_0 - \rho_s U_s\right) \frac{\partial \alpha_1}{\partial x_1}\right.$$

$$- \rho_s V_s \zeta_2 + \frac{m}{R} \frac{\partial \mu_s}{\partial x_1} \frac{\partial \zeta_3}{\partial y} + \frac{f}{R} \mu_s \frac{\partial}{\partial x_1} \left(\frac{\partial \zeta_3}{\partial y}\right) + \frac{1}{R} \frac{\partial \mu_s}{\partial y} \frac{\partial \zeta_3}{\partial x_1} - \frac{\partial \zeta_4}{\partial x_1}$$

$$\left. + \left[\frac{i}{R} \alpha_0 \frac{d\mu_s}{dT_s} \left(r \frac{\partial U_s}{\partial x_1} + m \frac{\partial V_\rho}{\partial y}\right) - \frac{d\rho_s}{dT_s} \left(U_s \frac{\partial U_s}{\partial x_1} + V_s \frac{\partial U_s}{\partial y}\right)\right] \zeta_5\right\} A,$$

$$I_y = \left[\frac{m}{R}\frac{\partial \mu_s}{\partial y}\zeta_1 + \frac{f}{R}\mu_s\zeta_2 + \left(\frac{2i}{R}\mu_s\alpha_0 - \rho_s U_s\right)\zeta_3 + \frac{1}{R}\frac{d\mu_s}{dT_s}\frac{\partial U_s}{\partial y}\zeta_5\right]\frac{dA}{dx_1}$$

$$+ \left\{\frac{m}{R}\frac{\partial \mu_s}{\partial y}\frac{\partial \zeta_1}{\partial x_1} + \frac{1}{R}\frac{\partial \mu_s}{\partial x_1}\zeta_2 + \frac{f}{R}\mu_0\frac{\partial \zeta_2}{\partial x_1} + \left[\frac{i}{R}\left(\mu_s\frac{d\alpha_0}{dx_1} + \alpha_0\frac{\partial \mu_s}{\partial x_1}\right)\right.\right.$$

$$\left. - \rho_s\frac{\partial V_s}{\partial y}\right]\zeta_3 - \rho_s V_s\frac{\partial \zeta_3}{\partial y} + \left(\frac{2i}{R}\mu_s\alpha_0 - \rho_s U_s\right)\frac{\partial \zeta_3}{\partial x_1} + \frac{1}{R}\left[f\frac{d\mu_s}{dT_s}\frac{\partial}{\partial x_1}\times\right.$$

$$\left(\frac{\partial U_s}{\partial y}\right) + \frac{\partial U_s}{\partial y}\frac{\partial}{\partial x_1}\left(\frac{d\mu_s}{dT_s}\right) + r\frac{d\mu_s}{dT_s}\frac{\partial^2 V_s}{\partial y^2} + \left(r\frac{\partial V_s}{\partial y} + m\frac{\partial U_s}{\partial x_1}\right)\frac{\partial}{\partial y}\left(\frac{d\mu_s}{dT_s}\right)\Big]\zeta_5$$

$$\left. + \frac{1}{R}\frac{d\mu_s}{dT_s}\frac{\partial U_s}{\partial y}\frac{\partial \zeta_5}{\partial x_1} + \frac{1}{R}\frac{d\mu_s}{dT_s}\left(r\frac{\partial V_s}{\partial y} + m\frac{\partial U_s}{\partial x_1}\right)\zeta_6\right\} A,$$

$$I_e = \left[\left(\frac{2i}{RPr_e c_{p_s}}\alpha_0\kappa_s - \rho_s U_s\right)\zeta_5\right]\frac{dA}{dx_1} - \left\{\rho_s\frac{\partial T_s}{\partial x_1}\zeta_1 - \left[\frac{i}{RPr_e c_{p_s}}\times\right.\right.$$

$$\left(\alpha_0\frac{d\kappa_s}{dT_s}\frac{\partial T_s}{\partial x_1} + \kappa_s\frac{d\alpha_0}{dx_1} + \alpha_0\frac{\partial \kappa_s}{\partial x_1}\right) - \left(\frac{d\rho_s}{dT_s} + \frac{\rho_s}{c_{p_s}}\frac{dc_{p_s}}{dT_s}\right)\left(U_s\frac{\partial T_s}{\partial x_1}\right.$$

$$\left. + V_s\frac{\partial T_s}{\partial y}\right)\Big]\zeta_5 + \left(\frac{2i}{RPr_e c_{p_s}}\alpha_0\kappa_s - \rho_s U_s\right)\frac{\partial \zeta_5}{\partial x_1} - \rho_s V_s\zeta_6\Big\} A.$$

APPENDIX III

The variation of the thermodynamic and transport properties with temperature is given by Lowell and Reshotko[5]

$$\rho^* = 1 - \frac{(T^* - 3.9863)^2(T^* + 288.9414)}{508929.2(T^* + 68.12963)} + 0.011445 \exp(-\frac{3.4.3}{T^*}),$$

ρ^* in gm/mℓ, T^* in °C.

$$\text{Log}(\frac{1.002}{\mu^*}) = \frac{1.37023(T^* - 20) + 8.36 \times 10^{-4}(T - 20)^2}{109 + T^*},$$

μ^* in C_p T^* in °C

$$\kappa^* = - 0.901090 + 0.1001982T^* - 1.873892 \times 10^{-4}T^{*2} + 1.039570 \times 10^{-7}T^{*3},$$

κ^* in megawatts $cm^{-1}K^{-1}$, T^* in °K.

$$c_p^* = 2.13974 - 9.68137 \times 10^{-3}T^* + 2.68536 \times 10^{-5}T^{*2} - 2.42139 \times 10^{-8}T^{*3},$$

c_p^* in cal $gm^{-1}K^{-1}$, T^* in °K .

Figure Captions

Figure 1. Variation of the spatial amplification rate with frequency at $x_{ref.}$ for power-law temperature distributions for $\Delta T = 2.78°C$ at $x_{ref.}$ using similar mean-flow profiles.

Figure 2. Power-law temperature distributions.

Figure 3. Variation of the spatial amplification rate with frequency at $x_{ref.}$ for the unheated case and the power-law temperature distributions of Fig. 2 for $\Delta T = 1.67°C$ at $x_{ref.}$ using nonsimilar mean-flow profiles.

Figure 4. Variation of the spatial amplification rate with frequency at $x_{ref.}$ for the unheated case and the power-law temperature distributions of Fig. 2 for $\Delta T = 2.78°C$ at $x_{ref.}$ using nonsimilar mean-flow profiles.

Figure 5. Variation of the spatial amplification rate with frequency at $x_{ref.}$ for the unheated case and the power-law temperature distributions of Fig. 2 for $\Delta T = 4.44°C$ at $x_{ref.}$ using nonsimilar mean-flow profiles.

Figure 6. Variation of the spatial amplification rate with streamwise position for the unheated case and the power-law temperature distributions of Fig. 2 for $\Delta T = 2.78°C$ at $x_{ref.}$ using nonsimilar mean-flow profiles.

Figure 7. Variation of the amplification factor with streamwise position for the unheated case and the power-law temperature distributions of Fig. 2 for $\Delta T = 2.78°C$ at $x_{ref.}$ using nonsimilar mean-flow profiles.

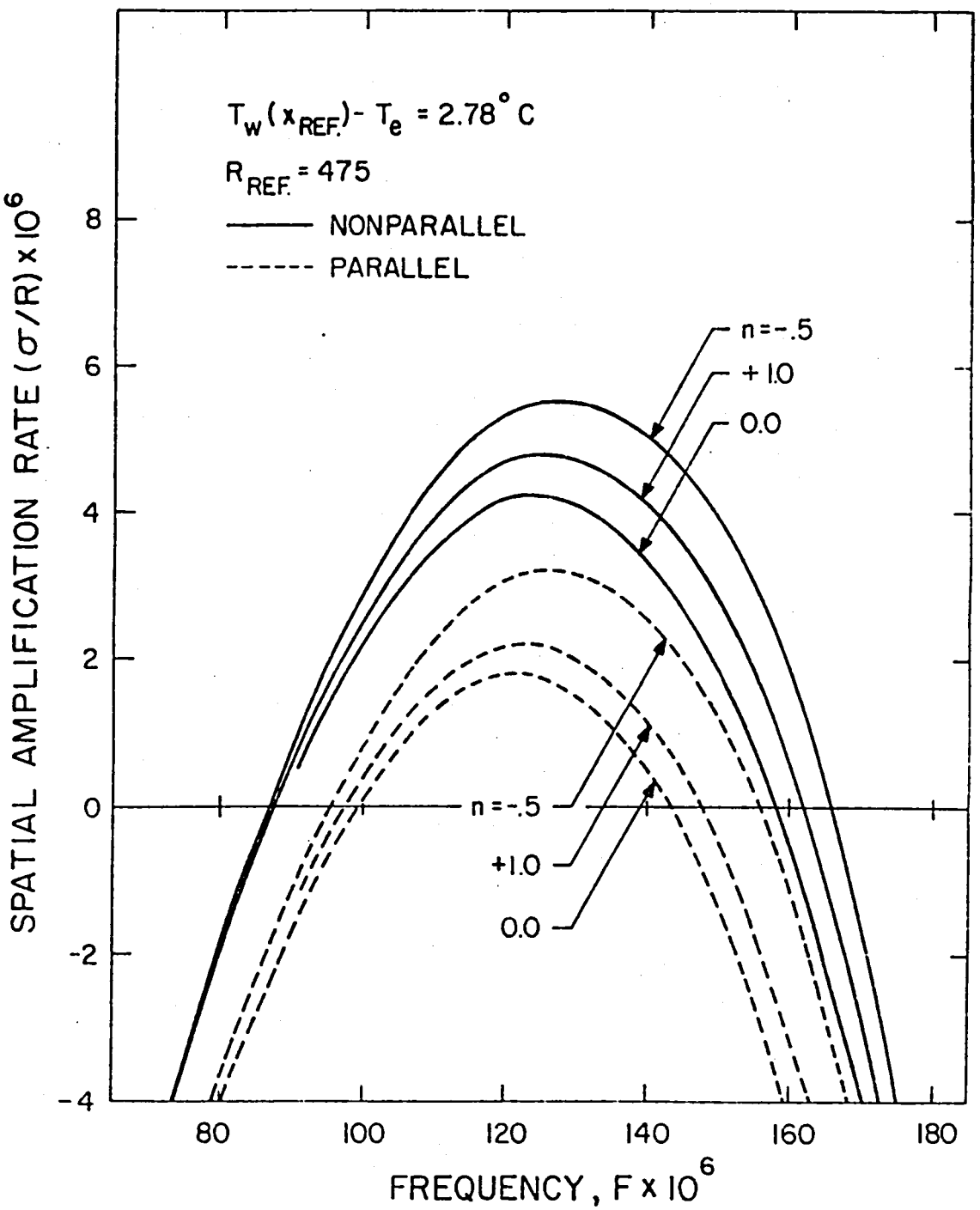

Figure 1. Variation of the spatial amplification rate with frequency at $x_{ref.}$ for power-law temperature distributions for $\Delta T = 2.78°C$ at $x_{ref.}$ using similar mean-flow profiles.

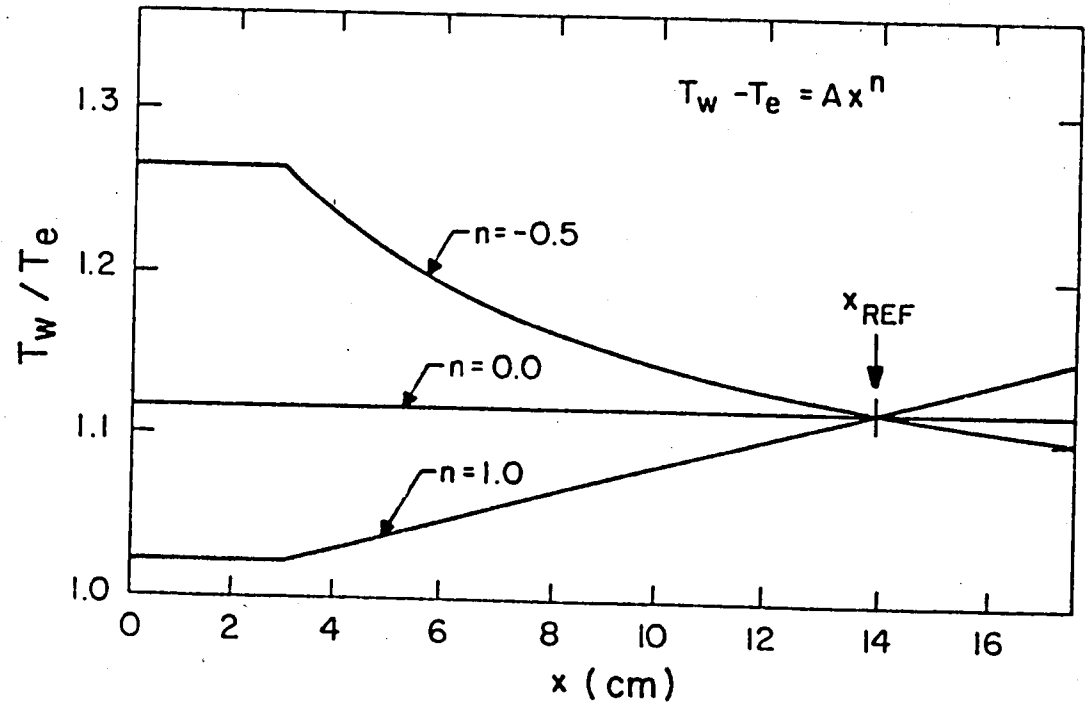

Figure 2. Power-law temperature distributions.

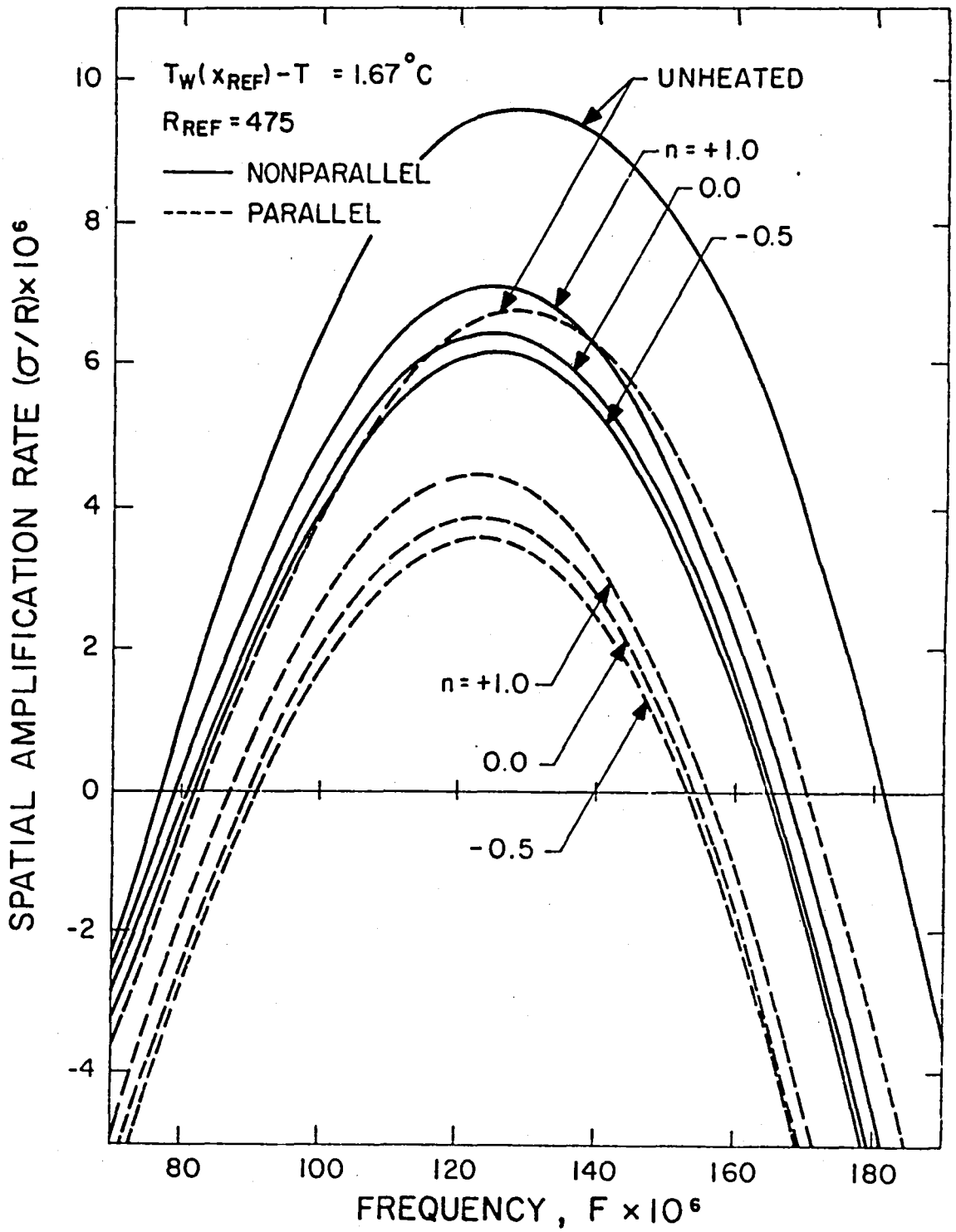

Figure 3. Variation of the spatial amplification rate with frequency at $x_{ref.}$ for the unheated case and the power-law temperature distributions of Fig. 2 for $\Delta T = 1.67°C$ at $x_{ref.}$ using nonsimilar mean-flow profiles

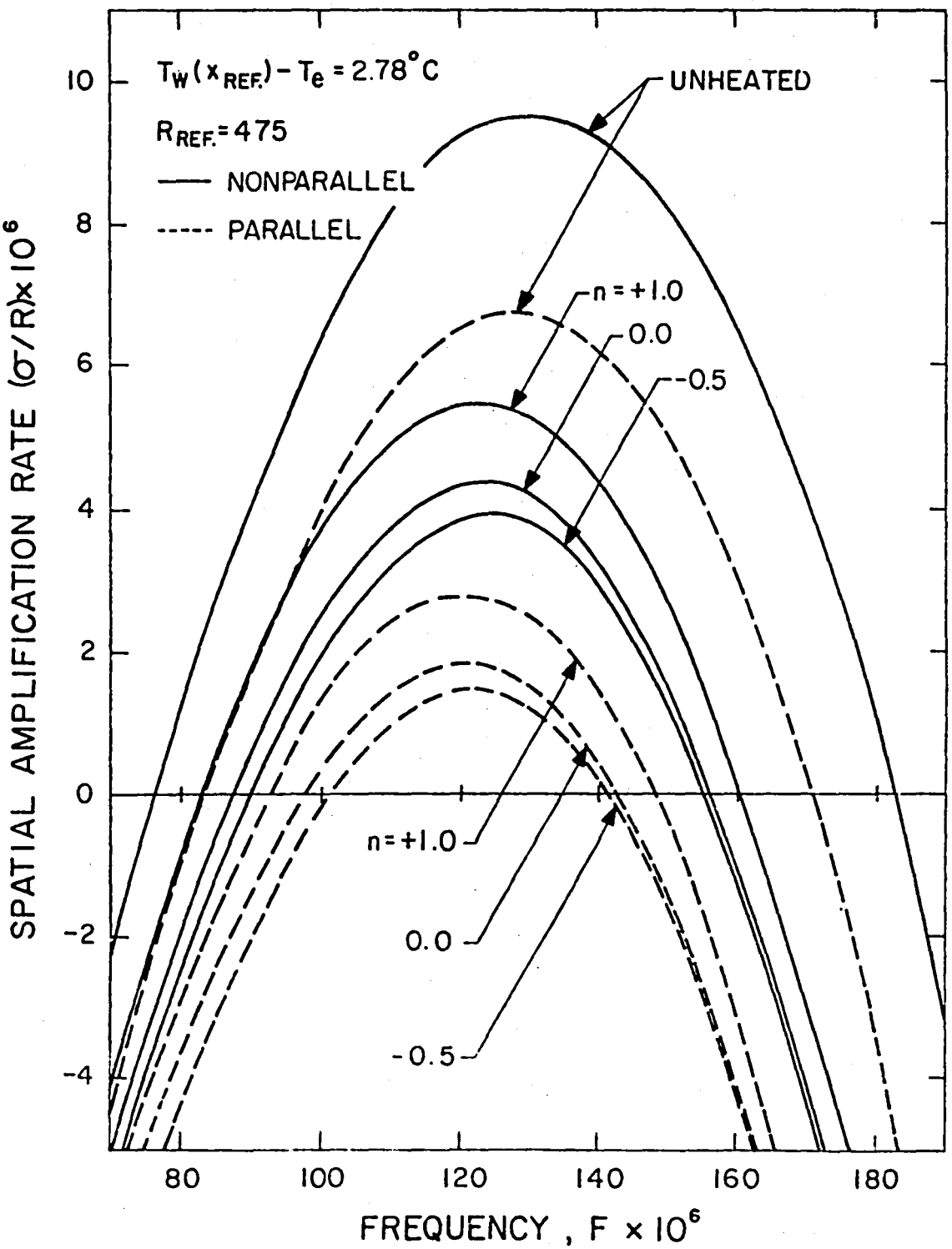

Figure 4. Variation of the spatial amplification rate with frequency at $x_{ref.}$ for the unheated case and the power-law temperature distributions of Fig. 2 for ΔT = 2.78°C at $x_{ref.}$ using non-similar mean-flow profiles.

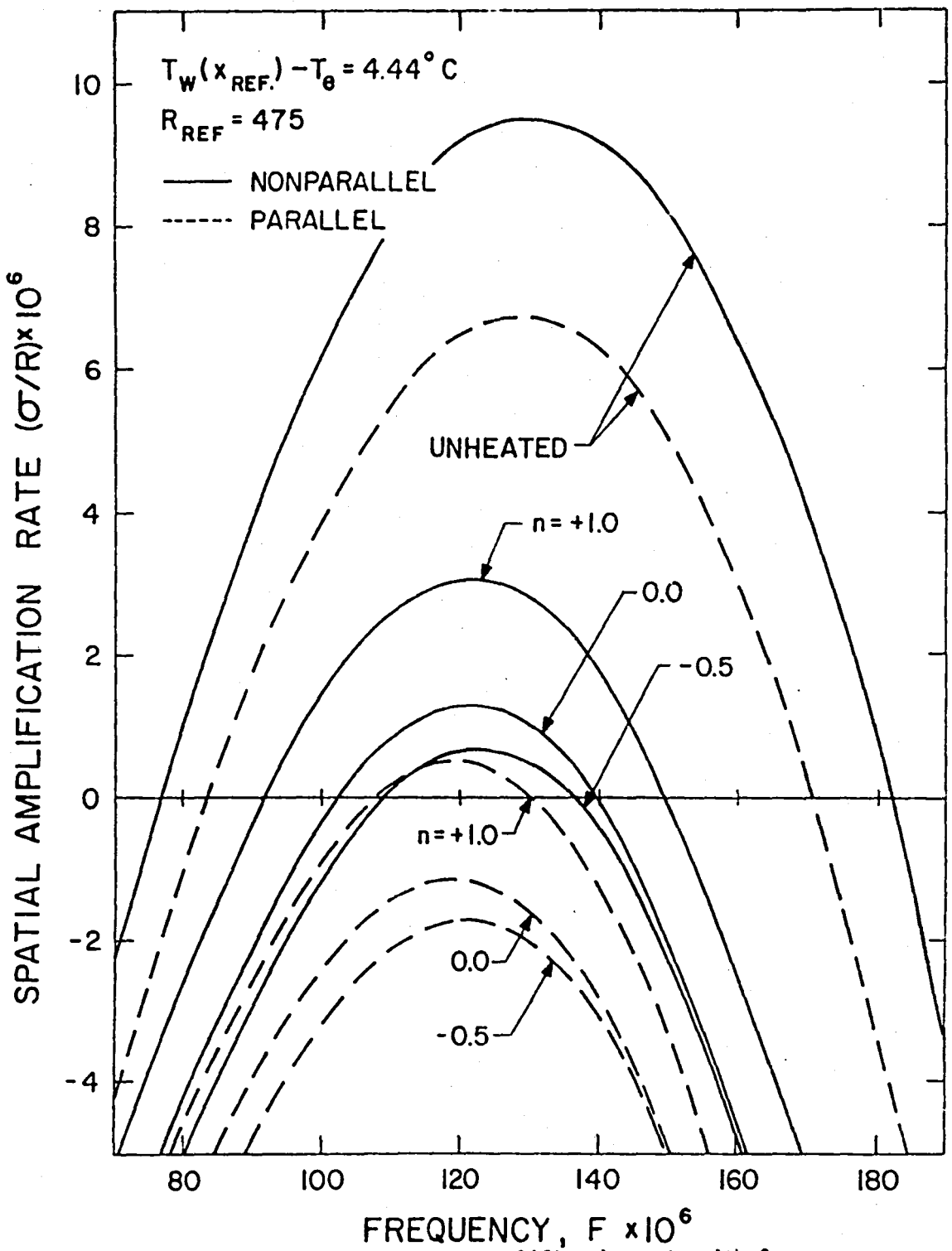

Figure 5. Variation of the spatial amplification rate with frequency at $x_{ref.}$ for the unheated case and the power-law temperature distributions of Fig. 2 for $\Delta T = 4.44°C$ at $x_{ref.}$ using non-similar mean-flow profiles.

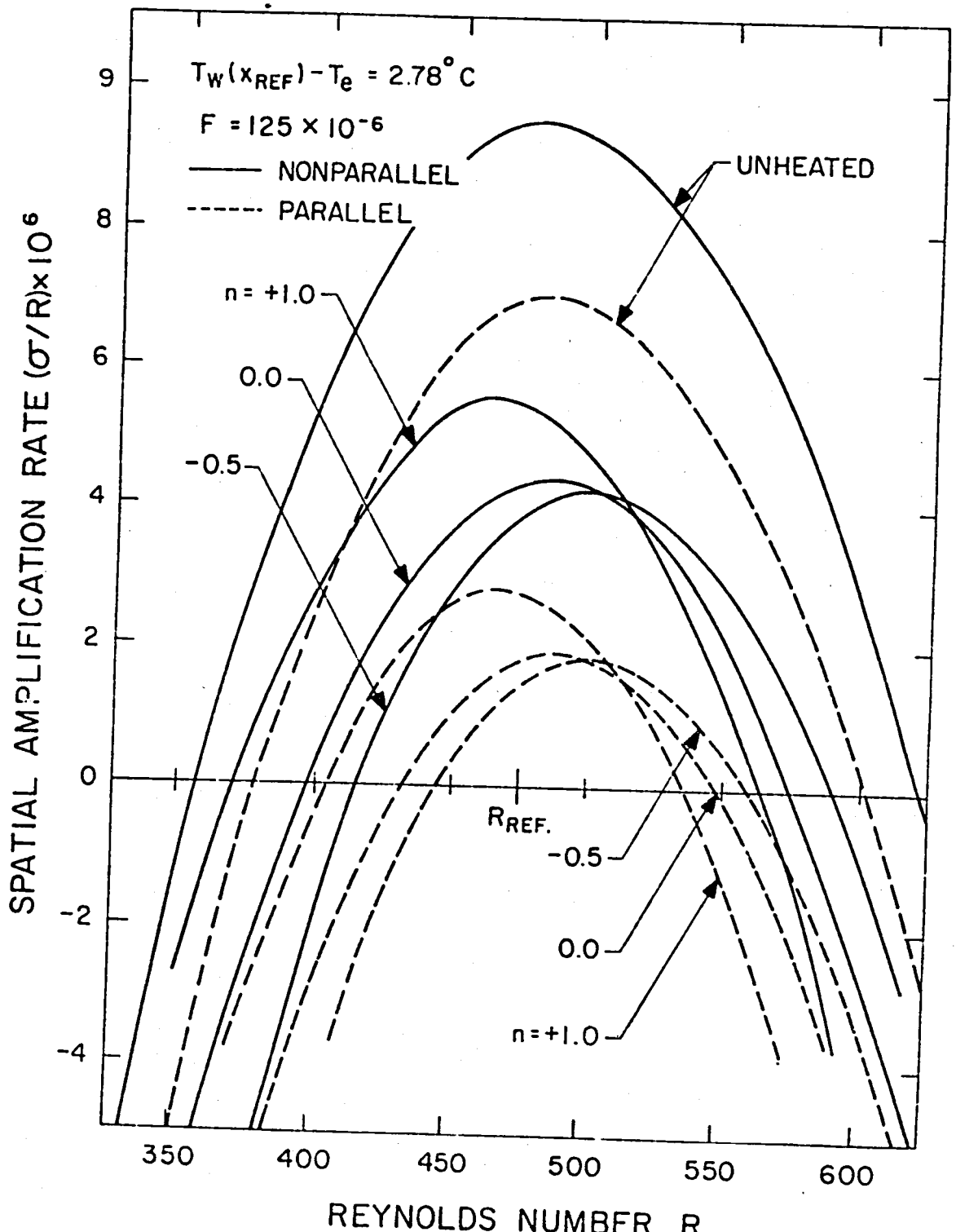

Figure 6. Variation of the spatial amplification rate with streamwise position for the unheated case and the power-law temperature distributions of Fig. 2 for $\Delta T = 2.78°C$ at $x_{ref.}$ using non-similar mean-flow profiles.

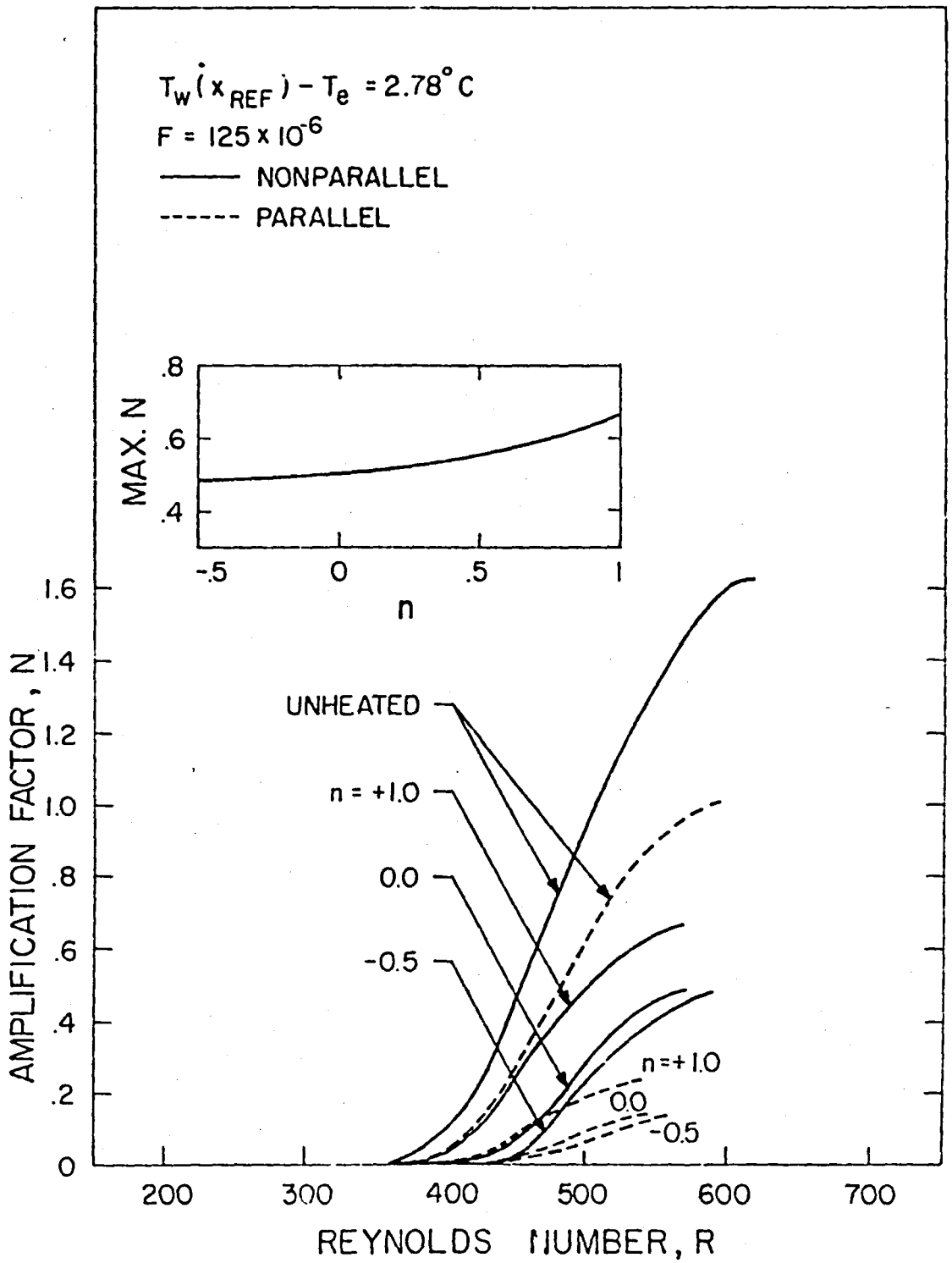

Figure 7. Variation of the amplification factor with streamwise position for the unheated case and the power-law temperature distributions of Fig. 2 for $\Delta T = 2.78°C$ at $x_{ref.}$ using non-similar mean-flow profiles.

END

DATE

FILMED

NOV 27 1979

End of Document